Scaling Laws in Granular Flow and Pedestrian Flow

Shumiao Chen[1], Fernando Alonso-Marroquin,[1*] Jonathan Busch,[1] Raúl Cruz Hidalgo,[2] Charmila Sathianandan[1], Álvaro Ramírez-Gómez,[3] and Peter Mora[4]

[1]*School of Civil Engineering, The University of Sydney, Sydney, NSW, Australia*
[2] *School of Applied Mathematics and Physics, The University of Navarra, Spain*
[3] *Polytechnic University of Madrid, Spain*
[4] *MCM Global, Sherwood Road, Toowong, Brisbane, QLD, Australia*

Abstract. We use particle-based simulations to examine the flow of particles through an exit. Simulations involve both gravity-driven particles (representing granular material) and velocity-driven particles (mimicking pedestrian dynamics). Contact forces between particles include elastic, viscous, and frictional forces; and simulations use bunker geometry. Power laws are observed in the relation between flow rate and exit width. Simulations of granular flow showed that the power law has little dependence on the coefficient of friction. Polydisperse granular systems produced higher flow rates than those produced by monodisperse ones. We extend the particle model to include the main features of pedestrian dynamics: thoracic shape, shoulder rotation, and desired velocity oriented towards the exit. Higher desired velocity resulted in higher flow rate. Granular simulations always give higher flow rate than pedestrian simulations, despite the values of aspect ratio of the particles. In terms of force distribution, pedestrians and granulates share similar properties with the non-democratic distribution of forces that poses high risks of injuries in a bottleneck situation.

Keywords: Pedestrian flow, granular flow
PACS: 05.10.-a

INTRODUCTION

Granular flow in a bottleneck occurs in many scenarios, such as gravity discharge in silos, block caving, transport of granular material in conveyor belts, traffic flow, and escape dynamics of pedestrians. The forces produced through the interactions between particles in granular flow are similar to the physical contact between pedestrians in panic-driven situations. The power law that relates the width of the exit to the flow rate of pedestrians is analogous to the Beverloo relation used in silos [10]. Placing an obstacle before the outlet can increase the flow rate in an hourglass [2]. This occurs not only in silos but also in the social force model for pedestrians [4]. and the escape dynamics of panicking ants [9]

Unlike bodies in granular flow, pedestrians are self-driven as opposed to gravity-driven; however there are still similarities between the behavior of pedestrians and granulates. Gravity defines both the desired acceleration and the direction of the pedestrians**,** and the terminal velocity for grains is analogous to the desired velocity of self-driven pedestrians. In this paper, we investigate to what extent the flow in granular materials can mimic the motion of pedestrians in a panic-driven situation. We present a model that allows us to compare granular flow (gravity-driven flow) to pedestrian flow (velocity-driven flow).

THE MODEL

The numerical study conducted in this paper will build upon ideas concerning contact forces between pedestrians in the social force model for panicking individuals [5]. The velocity $\vec{v}_i$ of a pedestrian *i* can be determined according to Newton's second law

$$\vec{F}_i = m_i \frac{d\vec{v}_i}{dt} , \quad (1)$$

where t is the time, m_i is the mass of the pedestrian and $\vec{F}_i$ is the force acting on the pedestrian.

$$\vec{F}_i = \vec{F}_i^0 + \sum_{j^1 i} \vec{F}_{ij} . \quad (2)$$

The first term on the right side in Eq. (2) denotes the self-driven component of a pedestrian's motion

$$\vec{F}_i^0 = \frac{v_0 \vec{e}_i - \vec{v}_i}{\tau} , \quad (3)$$

where τ is the time required by the pedestrian to reach maximal velocity, and v_0 is the desired speed.

The unit vector $\vec{e}_i$ is the desired direction of motion of the pedestrian. The self-driven force is equivalent to a force experienced by a gravity-driven particle in a viscous fluid. Using this analogy, we

Powders and Grains 2013
AIP Conf. Proc. 1542, 157-160 (2013); doi: 10.1063/1.4811891

defined gravity as $g=v_0/\tau$ and the coefficient of viscosity as $\gamma=1/\tau$, so that $\gamma=g/v_0$.

The second term on the right side in Eq. (2) is the sum of all interactions with other pedestrians, walls, columns, and obstacles. Each interaction force is calculated as

$$\vec{F}_{ij}=\vec{F}_{ij}^{e,n}+\vec{F}_{ij}^{e,t}+\vec{F}_{ij}^{v,n}+\vec{F}_{ij}^{v,t}, \quad (4)$$

where the elastic forces are given by

$$\vec{F}_{ij}^{e,n}=-k_n\delta_{ij}^n\vec{n}_{ij} \quad \vec{F}_{ij}^{e,t}=-k_t\delta_{ij}^t\vec{t}_{ij}, \quad (5)$$

and $\vec{n}_{ij}$ and $\vec{t}_{ij}$ are the normal and tangential unit vectors. The scalar δ_{ij}^n is the overlapping length and denotes the vertex to edge distance between the two particles [1]. The scalar denoted by δ_{ij}^t accounts for the tangential elastic displacement given by the frictional force, and it satisfies the sliding condition of $\left|\vec{F}_{ij}^{e,t}\right|\le\mu\vec{F}_{ij}^{e,n}$ where μ is the coefficient of friction. Here, k_n and k_t denote the normal and tangential coefficients of stiffness. The last two terms on the right hand side of Eq. (4) account for the coefficient of restitution between pedestrians (Alonso-Marroquín and Wang, 2009).

$$\vec{F}_{ij}^{v,n}=-m_{ij}\gamma_n v_{ij}^n\vec{n}_{ij} \quad \vec{F}_{ij}^{v,t}=-m_{ij}\gamma_t v_{ij}^t\vec{t}_{ij}, \quad (6)$$

where $m_i=\rho A_i$, the mass of the particle and $m_{ij}=m_i m_j/(m_i+m_j)$. The density is denoted by ρ, and A_i stands for the area of the 2D particle. The normal and tangential coefficients of viscosity are represented by γ_n and γ_t respectively; v_{ij}^n and v_{ij}^t denote the normal and tangential components of the contact velocity.

The parameters were chosen as follows: the thorax responses to forces $k_n=10^6$ N/m are taken from medical data on thorax deformation in response to forces (Bush, 2011); $k_t=10^5$ N/m leads to a bulk Poisson ratio of 0.3; $\mu=0.3$ is close to the coefficient of friction between pieces of cloth fabric. Given that there is so little information concerning restitution between pedestrians, so we chose $\gamma_n=40s^{-1}$ and $\gamma_t=0s^{-1}$, which correspond to normal and tangential coefficients of restitution of 0.3 and 1.0. The desired acceleration is $g=1m/s^2$ and the terminal velocity is $v_0=6m/s$. The surface density of the pedestrians is $\rho=10^3\,kg/m^2$. The diameter of the particles is d=0.3m.

Simulations were performed using sphero-cylinders, which represent the thoracic shape of the pedestrians. We compared two different models: the first one used granular particles driven by gravity only; the second model involves rotational dynamics consistent with the desired pedestrian orientation (that is, the line of the shoulders was perpendicular to the direction of motion). In the pedestrian model the particles were impelled by a self-driven force oriented towards the exit. The pedestrian model is depicted in Figure 1.

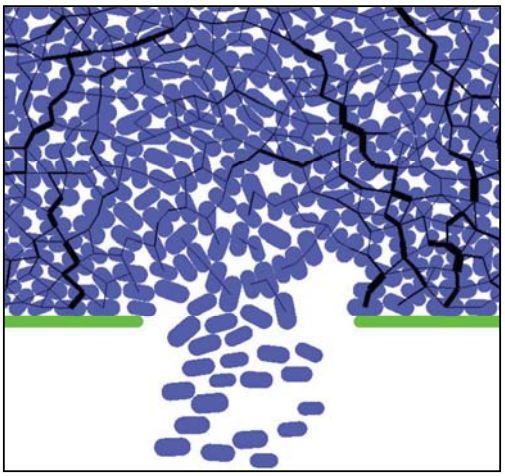

FIGURE 1. Snapshot of an advanced SPOLY model for pedestrian flow that incorporates the shape of the thorax and rotational dynamics. The black lines represent the magnitude of the forces between pedestrians.

The in-house computer program SPOLY was used to conduct the simulations. SPOLY is an object-oriented design program that simulates systems of sphero-polygons interacting via contact forces using Newton's equations of motion. Details relating to the SPOLY code can be found in (Alonso-Marroquín and Wang, 2009).

RESULTS

Simulations were performed to investigate the dynamics of both pedestrian and granular flow. We used a cylindrical bunker with an orifice of diameter D, discharging free-flowing particles of diameter d. The size of the orifice was varied, and the flow rate was calculated.

Two sets of simulations dealt with the effect of uniformity of particles on flow rate. One set used monodisperse particles with particle diameter 0.36m – the area of a pedestrian's thorax. The other set of simulations used polydisperse particles with diameters between 0.2m and 0.44m. Figure 2(b) shows that flow rates in polydisperse simulations are faster than those in the monodisperse simulations. It also shows that the difference in flow rates in the two sets of simulations increases as the exit size increases.

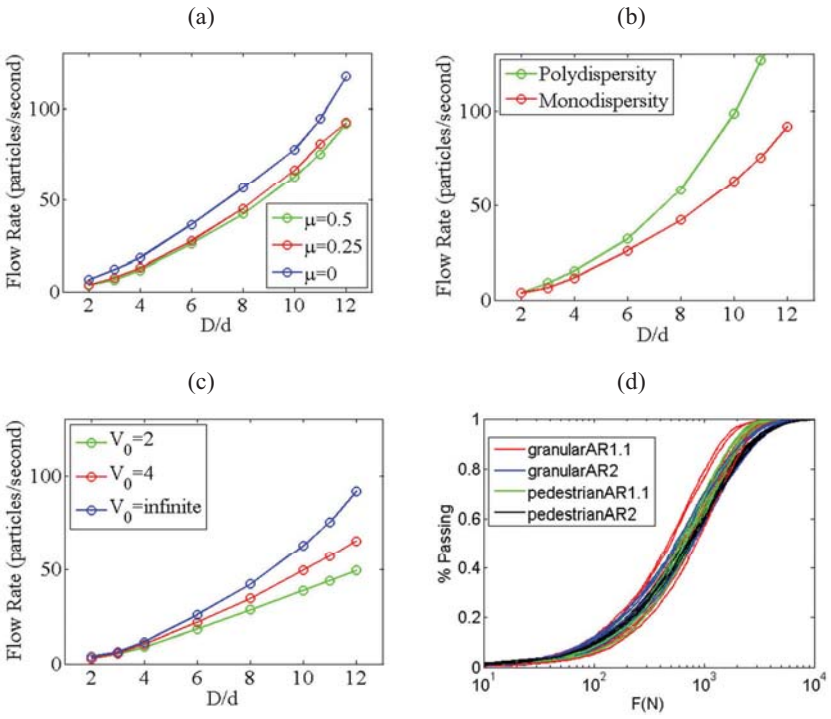

FIGURE 2. (a) Flow rate versus normalized exit width using monodisperse particles with different coefficient of friction. (b) Flow rate versus normalized exit width for polydisperse and monodisperse particles. (c) Flow rate versus normalized exit width for different terminal velocities (in m/s). (d) Cumulative distributions of contact forces between pedestrians using the four models: granular and pedestrian simulations with particles' aspect ratio of 1.1 and 2. The distributions at ten different times are superimposed in the figure.

Figure 2(a) shows flow rate as a function of the normalized width of the orifice for various values of the coefficient of friction. An interesting observation is the near independence of the flow rate on the coefficient of friction when $\mu \neq 0$. The plots for $\mu=0.25$ and $\mu=0.5$ are similar, indicating that the influence of coefficient of friction is minimal. If friction forces are absent, the flow rate increases. This is the case of non-panicking pedestrians, which allows some private space between them and therefore avoids friction forces between them.

Pedestrians' desired velocity v_0 depends on their level of panic. To investigate its effect on flow rate, we ran simulations with different v_0 by changing the coefficient of viscosity $\gamma=g/v_0$. The simulations were monodisperse, with exit width increased by fractions of 0.36m. Figure 2(c) shows that pedestrians who are panic less (lower v_0) produce a lower flow rate. This is consistent with the viscous properties of granular flow; but it does not capture the *faster-is-slower* effect obtained with other pedestrian models [8], which predict that if pedestrians increase their desired velocity, the overall flow rate declines. When pedestrians are not in a panic situation, private space between them is maintained; but in a panic situation private space is denied and friction is created between pedestrians, resulting in slower crowd movement. This is demonstrated in Figure 2(a): where private space is allowed ($\mu=0$), the flow rate is much greater than when private space is denied ($\mu \neq 0$). This may be the main reason behind the *faster-is-slower* effect; but confirmation of this hypothesis would need a more advanced model.

To investigate the effect of particle shape on the "safety" of pedestrians, we performed simulations with two different aspect ratios using both granular material and pedestrians. In the four simulations the exit width was 2.73m.

Table 1. Flow rates resulting from granular and pedestrian simulations with particles of differing aspect ratio.

	Aspect Ratio = 1.1	**Aspect Ratio = 2.0**
Granular	26.0046	24.0638
Pedestrian	25.7880	19.1925

Table 1 displays the flow rates calculated as particles crossing the exit per second. In both granular and pedestrian simulations, particles with an aspect ratio 1.1 have higher flow rate than those with aspect ratio 2. The pedestrian simulations, which included the fact that pedestrians eagerly want to move towards the exits, resulted in smaller flow rates than those generated by granular simulations. The contact network between the particles, shown in Figure 1 as an example, demonstrates that the forces on particles are non-democratic, as their distribution is neither uniform nor orderly. When applied to pedestrian motion, the contact forces can determine which pedestrians suffer the largest forces and are most likely to choke. At any

given point, a few pedestrians bear enormous forces. Some experience minor forces, while others feel no force. However, from Figure 2(d) it can be seen that this is a continuously changing dynamic varying with time. In Figure 2(d) we also see the percentage of pedestrians who are "safe" ($F<10^2$N), "in danger" (10^2N$<F<10^3$N), "severely injured" (10^3N$<F<10^4$N), or "dead" ($F>10^4$N).

CONCLUSIONS

Flow rate analysis from the simulations has led to an extension of the Beverloo Relation for bottlenecks. The Beverloo Relation for granular flow was extended to create a generalized power law that can be applied to pedestrian-like particles. It was found that the Beverloo relation holds for gravity-driven pedestrians. The simulations produced a power-law relation between 1.4 and 1.7, which is consistent with the 3/2 determined by the momentum analysis using the Hourglass Theory [7] and dimensional analysis [6] By examining the effects of the coefficient of friction on the Beverloo Relation, it was confirmed that when $\mu \neq 0$, the effect of changing the coefficient of friction is negligible – as suggested by The Hour-Glass Theory (Nedderman, 1992). Upon verifying that the model used in this paper supports the Beverloo relation, the parameters of the simulation were adjusted to represent pedestrian-like particles. For these adjusted particles the simulations indicated a substantial deviation from the Beverloo Relation, as the power law produced had an exponent of 1.9 ± 0.1 rather than 3/2. Calculating flow rates demonstrated a positive correlation between the desired velocity of the pedestrians and observed flow rates, indicating that contact forces are not enough to reproduce the *faster-is-slower* effect. We suggest that this effect comes from "social" interactions between the pedestrians, and that future advancement of the model to incorporate the psychological avoidance behavior inherent in pedestrian motion would enable the program to be valid for normal situations of pedestrian motion. This can be introduced using an extra random, repulsive force similar to the one proposed by Helbing et al. [5] These advances will allow for the determination of the factors to produce the *faster-is-slower* effect observed in earlier literature.

ACKNOWLEDMENTS

The project is supported by The University of Sydney Civil Engineering Research Funding Scheme (CERDS)

REFERENCES

1. Alonso-Marroquín, F., and Y. Wang *Granular Matter* **11**: 317–329(2009),.
2. Alonso-Marroquin, F., S. Azeezullah, S. A. Galindo-Torres, and M. L. Kettle-Olsen, *Phys. Rev. E* **85**, 020301(R) (2012).
3. Bush, J., "A Realistic Discrete Element Model of Pedestrian Panic Behaviour," honors thesis, The University of Sydney, 2011.
4. Escobar, R., and A. De La Rosa (2003), in *Advances in Artificial Life*, ed. W. Banzhaf, T. Christaller, P. Dittrich, J. T. Kim, and J. Ziegler, Springer-Verlag, Berlin, 97–106.
5. Helbing, D., B. Lubos, J. Anders, and W. Torsten, , *Transportation Science* **39**: 1–24 (2005).
6. Mankoc, C., A. Janda, R. Arevalo, J. M. Pastor, I. Zuriguel, A. Garcimartin, and D. Maza, *Granular Matter* **9**: 407–414 (2007).
7. Nedderman, R. M., *Statics and Kinematics of Granular Materials*, Cambridge: Cambridge University Press, 1992.
8. Parisi, D. R., and C. O. Dorso, *Physica A* **385**: 343–355 (2007).
9. Shiwakoti, N., M. Sarvi, G. Rose, and M. Burd, *Journal of the Transportation Research Board* **2137**: 31–37 (2009).
10. Tajima, Y., K. Takimoto, and T. Nagatani, *Physica A*, 294: 257–268 (2001).